Regular Surface Patterns on Rayleigh-Taylor Unstable Evaporating Films Heated from Below

Michael Bestehorn and Domnic Merkt

Lehrstuhl für Theoretische Physik II, Brandenburgische Technische Universität, Erich-Weinert-Strasse 1, 03046-Cottbus, Germany

(Received 4 May 2006; published 18 September 2006)

We study a thin liquid film with a free surface on the underside of a cooled horizontal substrate. We show that if the fluid is initially in equilibrium with its own vapor in the gas phase below, regular surface patterns in the form of long-wave hexagons having a well-defined lateral length scale are observed. This is in sharp contrast to the case without evaporation where rupture or coarsening to larger and larger patterns is seen in the long time limit. In this way, evaporation could be used for regular structuring of the film surface. Finally, we estimate the finite wave length for the simplified case of an extended Cahn-Hilliard equation.

DOI: 10.1103/PhysRevLett.97.127802 PACS numbers: 68.15.+e, 47.20.Ma, 64.70.−p, 68.55.−a

Surface patterns of thin liquid films on a solid support were studied during the last decade in numerous experimental and theoretical contributions (see [1–8] and references therein). In coating or wetting processes, a plane surface is usually desirable and the formation of surface deflections should be avoided. In contrast in modern (nano-) technological applications the creation and control of ordered structures come more and more into the focus of interest. Liquid thin films are applied in different ways to produce patterns with prescribed length scales and geometries. One possibility is to use a structured substrate [1,2]. In the present Letter we wish to concentrate on another method: the self-organized pattern growth due to an instability mechanism of the initially flat film [3,4]. There are several mechanisms that may destabilize a flat surface and allow us to control the growth of surface patterns. Flat ultrathin films may become unstable by van der Waals forces between surface and substrate [5–7]. Thicker films can be destabilized by inhomogeneous tangential surface tensions, which in turn are often caused by lateral gradients of temperature and/or, in mixtures, of concentration [8–12]. A rather simple method for destabilization is to put the film upside down, i.e., to position it under a flat horizontal plate. Then gravity acts against the stabilizing surface tension and inhomogeneous surface patterns result [13]. This is called Rayleigh-Taylor instability (RTI).

Up to now, most of the theoretical work is based on an interface equation, often called thin film equation, describing the location $z = h(x, y, t)$ of the free surface of the liquid [3,14–16]. This equation can be derived from the Navier-Stokes equation using the lubrication approximation. Additional effects caused by (moderate) evaporation or condensation on the interface can be included easily in the formalism [17,18]. Previous work shows that in the case of a surface-driven thermal instability, rupture of the film occurs after a relatively short time [11,19,20]. Rupture means that the surface function h reaches zero. From that moment on the thin film equation is meaningless since points occur where h is no longer differentiable. To avoid rupture, a repelling short range interaction can be introduced. Then patterns in the long time limit may be studied and show coarsening, a slow increase of the lateral dimensions of the structures (drops or holes) until one big hole (or drop) eventually remains [12].

In the present Letter, we shall concentrate on the Rayleigh-Taylor instability as destabilizing mechanism of the flat surface. In addition we assume a vertical heat gradient applied from outside. Further we neglect the dependence of surface tension on temperature as well as convective heat transfer in both layers. If the fluid is heated from below, this usually would stabilize the flat film. As was shown in [13], RTI may occur if the temperature gradient is not too large and film rupture is avoided by the stabilizing Marangoni effect.

In previous works, evaporation was considered as a destabilizing mechanism. Here we shall concentrate on the opposite case. Assume that the fluid is heated from below (or cooled from above). If the partial pressure of the vapor in the gas layer under the fluid is equal to the saturation pressure belonging to the surface temperature of the initial flat film, then a small elevation of the surface into colder regions leads to local condensation, a small depression into hotter regions causes evaporation (Fig. 1). We show that this mechanism may avoid rupture for large

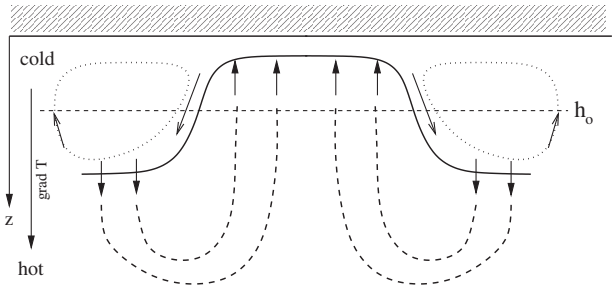

FIG. 1. If the surface of a fluid under a horizontal plate is heated from below and deflected around the value where the two phases are in equilibrium, thicker parts evaporate, thinner regions condensate. This stabilizing mechanism may be overcome by gravitation and an instability may occur.

enough evaporation rates even without the Marangoni effect. Moreover, due to the modified character of the instability, coarsening does no longer occur in the long time limit. Instead we find very regular cell structures in the form of hexagons, known from their morphology from small scale convection in thicker fluid layers [21–23].

Thin film dynamics with evaporation.—The spatiotemporal evolution of the location $z = h(x, y, t)$ of the surface of a thin film of an evaporating fluid is described by the kinematic boundary condition and the continuity equation [3]

$$\partial_t h = -\nabla_2 \int_0^{h(x,y,t)} \vec{v}_H dz - \frac{J}{\rho}. \tag{1}$$

Here, $\nabla_2 = (\partial_x, \partial_y)$, $\vec{v}_H$ denotes the horizontal components of the velocity field of the fluid and ρ its density which is assumed to be constant. The mass flux density J [in kg/(m^2 s)] measures the mass per second evaporating or condensing on a surface with area 1 m^2. In general, J is a complicated function of temperature, pressure, and fluid parameters. It can be roughly estimated using a Hertz-Knudsen law:

$$J(T, P_e) = \alpha(P_s(T) - P_v)\sqrt{\frac{m}{2\pi kT}}, \tag{2}$$

where P_s is the saturation pressure of the liquid, P_v the partial pressure of vapor in the atmosphere below the film, m the molecular mass of the fluid particles, and k Boltzmann's constant. The so-called accommodation coefficient α accounts for an adjustment of the real conditions at the surface on the idealized assumptions used for deriving the Hertz-Knudsen law. It must be less than 1 but, depending on the experimental situation, can be as small as $10^{-3} \ldots 10^{-6}$.

The temperature distribution in the fluid layer follows from the temperature equation, the boundary conditions $T(z = H) = T_b$, $T(z = 0) = T_u$, and interface conditions (Fig. 2):

$$\begin{aligned} &T(z = h - \epsilon) = T(z = h + \epsilon) = T_I, \\ &\lambda_1 \partial_z T|_{z=h-\epsilon} = \lambda_2 \partial_z T|_{z=h+\epsilon} - LJ, \qquad \epsilon \to 0, \end{aligned} \tag{3}$$

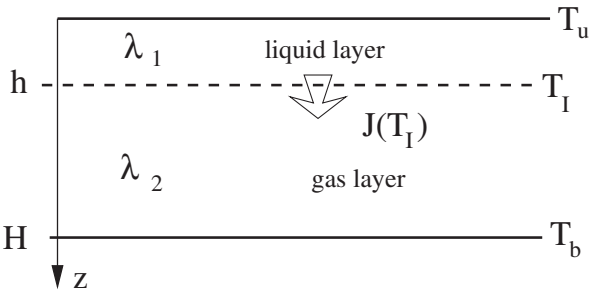

FIG. 2. Sketch of the system. The temperatures T_b and T_u are fixed, the interface temperature T_I depends on h. Evaporation or condensation causes a temperature dependent mass flux $J(T_I)$.

with λ_i as thermal conductivity of the fluid and the atmosphere and L as latent heat.

Applying the lubrication approximation, the temperature can be expressed as a linear function of z, varying slowly with the film thickness on the lateral scale. Using the temperature equation together with conditions (3), the surface temperature T_I follows implicitly from the equation

$$T_I\left(\frac{\lambda}{h} + \frac{1}{H - h}\right) = T_b \frac{\lambda}{h} + \frac{T_u}{H - h} - \frac{L}{\lambda_2} J(T_I) \tag{4}$$

with $\lambda = \lambda_1/\lambda_2$.

Now we wish to consider the case where the flat film is in equilibrium with its own vapor, i.e., its surface temperature is equal to the saturation temperature T_s following from $P_s(T_s) = P_v$. At equilibrium, we have $J(T_s) = 0$ and $T_I = T_s$. Solving (4) for h yields the equilibrium thickness h_0 of the film if T_u and T_b are fixed:

$$h_0 = \frac{H}{1 + a} \quad \text{with} \quad a = \frac{T_b - T_s}{\lambda(T_s - T_u)}. \tag{5}$$

Since the film is assumed to be very thin compared to the air layer below we have $h_0 \ll H$ and thus $a \gg 1$ and therefore $h_0 \approx H/a$. For simplicity we neglect in the following the latent heat in (4) and put $L = 0$. Then we can solve (4) for T_I and expand it to the first order in h. Subtracting T_s we find

$$T_I - T_s \approx (T_s - T_u)\frac{h - h_0}{h_0}, \tag{6}$$

and, expanding (2) with respect to $T_I - T_s$ a linear relation between evaporation rate and film thickness results

$$J(T_I) \approx \tilde{\alpha}(T_s - T_u)\frac{h - h_0}{h_0}, \tag{7}$$

where the temperature difference vertically along the film enters as a control parameter. For $\tilde{\alpha}$ one finds $\tilde{\alpha} = \alpha(m/2\pi kT_s)^{1/2}(dP_s/dT)_{T_s}$. For water with T_s at room temperature one finally has $\tilde{\alpha} \approx \alpha \times 0.13$ Kg/(m^2 s K).

Using again the lubrication approximation, the horizontal velocity of the film is expressed as a function of the thickness h. For the conserved part of (1) one may write

$$\nabla_2 \int_0^{h(x,y,t)} \vec{v}_H dz = \nabla_2\left[-\frac{h^3}{3}\nabla_2 P(h) + \frac{h^2}{2}\nabla_2 \Gamma(T_I)\right], \tag{8}$$

which is found from integrating the Stokes equation [3]. Here $P(h)$ describes the (disjoining) pressure for which several models have been investigated in the recent literature, and $\Gamma(T_I)$ denotes the surface tension, which depends in general on the surface or interface temperature T_I of the film. For the following we assume only gravity and Laplace pressure on the interface, i.e., $P(h) = -\rho g h - \Gamma\Delta_2 h$, and neglect the dependence of Γ on temperature.

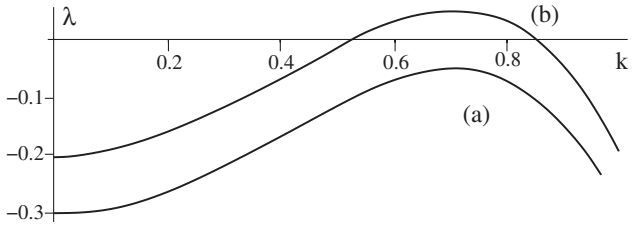

FIG. 3. Growth rates of waves with wave number k for (a) $E = 0.3$, (b) $E = 0.2$. Pattern formation occurs for (b).

Scaling of the horizontal coordinates by the capillarity length $l = \sqrt{\Gamma/\rho g}$, depth by the initial fluid depth d, and time by $\tau = 3\Gamma\eta/(\rho^2 g^2 d^3)$, one finds from (1) the dimensionless governing equation:

$$\partial_t h = -\nabla_2\{(h^3 + h^3\Delta_2)\nabla_2 h\} - E(h-1). \tag{9}$$

Here, E is an evaporation number defined as

$$E = \frac{\tilde{\alpha}\tau}{\rho}\frac{T_I - T_u}{d}. \tag{10}$$

Linear stability analysis of (9) shows that the flat film with depth $h = 1$ is unstable with respect to plane waves with wave number k if $E < k^2 - k^4$. If the fluid is heated from above ($E < 0$) this is always the case for small enough k. If the film is in the beginning in its equilibrium thickness h_0 [Eq. (5)] with $T_I = T_S$, any small disturbance will lead to complete evaporation or condensation, i.e., $h = h_0$ is unstable to long-wave modes.

Cooled from above: Numerical simulations.—If the film is cooled from above, $E > 0$ and a pattern forming instability occurs as long as $E < E_c = \frac{1}{4}$. Then patterns with the critical wave number $k_c^2 = 1/2$ become first unstable. The spectrum (Fig. 3) resembles that of small scale convective instabilities. Numerical solutions in two dimensions show that in contrast to the nonevaporating case there is no coarsening in the long-time limit. Instead, patterns with a length scale having the critical wave length as a lower bound are found forming *regular stationary* structures in the form of hexagons (Fig. 4). The value of E seems not to be very important for the qualitative behavior. It has just to be large enough to avoid film rupture.

Water as a working substance.—To give an impression of the time and length scales of the system we use water at 60 °C for the liquid layer with depth $d = 10^{-4}$ m. With $\Gamma = 6.6 \times 10^{-2}$ N/m, $\eta = 4.7 \times 10^{-4}$ kg/ms, $\kappa = 1.6 \times 10^{-7}$ m/s^2 one finds $l = 2.6$ mm and $\tau = 0.97$ s. An evaporation number of 0.2 used for the run of Fig. 4 would be reached with a temperature difference (in K) of $T_I - T_u = 0.15/\alpha$, which should be feasible even for α much less then one.

To estimate the influence of convective heat transfer which is neglected in our approach, one has to compute the ratio of $|dT/dt|$ and $|\kappa\Delta T|$. Assuming a typical (smallest) length Λ of the structures and a time scale τ, one finds

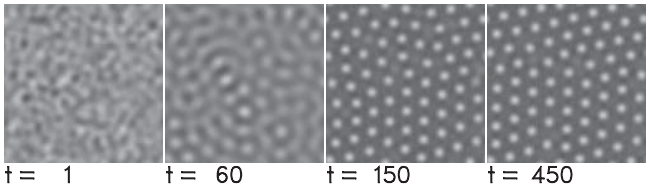

FIG. 4. Time series found by numerical integration of Eq. (9) with $E = 0.2$. Resolution 128×128 points, side length 80 capillary lengths. For larger values of E close to $1/4$ the final patterns are even more regular.

$$r = \frac{1}{\tau}\Big/\frac{\kappa}{\Lambda^2}.$$

If $r \ll 1$, convective heat transport can be neglected compared to heat diffusion. Doing the computation for the water layer, one finds for $\Lambda = d = 10^{-4}$ m a value of $r \approx 0.06$. The air layer is thicker, which slows down heat diffusion. On the other hand κ is much larger. Using $\Lambda = 10^{-3}$ m and $\kappa = 2.7 \times 10^{-5}$ m/s^2, we have still $r = 0.25$. If a fluid with a higher viscosity is used, this increases τ (for a 50 cS silicone oil one gets $\tau \approx 25$ s) and decreases r, so at least for viscous fluids the neglect of convection can be justified.

Free energy functional.—It is well known that for $E = 0$ (9) can be derived from a functional $F[h]$ that monotonically decreases in time [12]:

$$\partial_t h = \nabla_2\left\{h^3\nabla_2\left(\frac{\delta F[h]}{\delta h}\right)\right\}. \tag{11}$$

It can be shown that the minimum of F coincides with the structure having the lowest surface energy and therefore the smallest surface. This is why coarsening occurs [24].

But even for the case $E \neq 0$ such a free energy can be constructed. For (9) it has a rather complicated nonlocal form and will be presented elsewhere. Here, we shall discuss the extended Cahn-Hilliard equation, which also shows coarsening for $E = 0$, as a simplified model [25]:

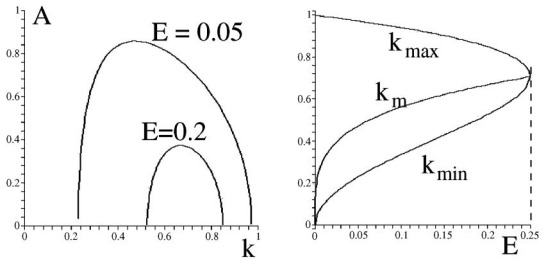

FIG. 5. Extended Cahn-Hilliard Eq. (12). Left: amplitude of a stationary sinusoidal surface deflection as function of its wave vector for two values of E. Right: The mode with largest amplitude has the wave vector k_m. For $E > 1/4$ only the trivial solution $u = 0$ is stable.

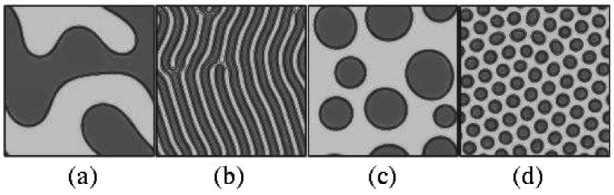

FIG. 6. Patterns found by numerical integration of the extended Cahn-Hilliard Eq. (12) after $T = 5000$, side length 100 [in units of (12)]. (a),(b) $u_0 = 0$. Without evaporation [$E = 0$, (a)], mazes are found after coarsening. With evaporation [$E = 0.2$, (b)] parallel oriented stripes are formed. (c),(d) $u_0 = 0.2$. Coarsening drops for $E = 0$ (c) and regular hexagons for $E = 0.1$ (d). Numerical resolution 128×128 points.

$$\partial_t u = -\epsilon\Delta u - \Delta^2 u + \Delta(u^3) - \epsilon^2 E(u - u_0) = \Delta\left(\frac{\delta F[u]}{\delta u}\right). \tag{12}$$

For (12) one computes for the case $u_0 = 0$

$$F[u] = F_{\mathrm{GL}}[u] - \frac{1}{2}\epsilon^2 E \iint G(\vec{r} - \vec{r}')u(\vec{r})u(\vec{r}')dV dV', \tag{13}$$

with the Ginzburg-Landau free energy F_{GL} and G as the potential of a point charge $\Delta G(\vec{r}) = \delta(\vec{r})$. A stationary solution of (12) corresponding to parallel stripes is given in lowest order of ϵ by $u = A\epsilon^{1/2}\sin(\epsilon^{1/2}kx)$, with the amplitude

$$A^2 = \frac{4}{3}(1 - k^2 - E/k^2). \tag{14}$$

The amplitude is real in the domain $k_{\min} < k < k_{\max}$ (Fig. 5) and has an upper bound with respect to wavelength if $E \neq 0$. The maximum of A is located at $k_m = E^{1/4}$, corresponding to the wavelength $\lambda_m = 2\pi\epsilon^{-1/2}E^{-1/4}$. It can be easily shown that for $k = k_m$ the functional (13) has its absolute minimum. Since the dynamics of (12) is variational, the finally selected patterns will have wave vectors with modulus close to $\epsilon^{1/2}k_m$. In the same way the stability of the different symmetries of the stationary solutions (rolls, hexagons, or even squares for more complicated nonlinearities) could be checked.

Figure 6 finally shows patterns after a long integration time of Eq. (12). Depending on the values of E and u_0, stripes, hexagons, mazes, or coarsening drops are obtained.

In conclusion, it is important to note that the hexagons found by numerical integration of the thin film equation with evaporation are still on a large scale compared to the layer depth. Although looking similar to the classical small scale structures obtained in Bénard-Marangoni convection, the behavior of the thin film fluid is completely different. Deformation plays a crucial role, whereas for small scale structures the surface can be assumed to be flat in a good approximation.

We thank S. Van Vaerenbergh, ULB Brussels, Belgium, for helpful discussions on thermal properties of binary mixtures.

[1] N. Rehse *et al.*, Eur. Phys. J. E **4**, 69 (2001).
[2] L. Rockford *et al.*, Phys. Rev. Lett. **82**, 2602 (1999).
[3] A. Oron, S. H. Davis, and S. G. Bankhoff, Rev. Mod. Phys. **69**, 931 (1997).
[4] A. Pototsky, M. Bestehorn, and U. Thiele, Physica D (Amsterdam) **199**, 138 (2004).
[5] G. Reiter *et al.*, Langmuir **15**, 2551 (1999).
[6] G. Reiter, Phys. Rev. Lett. **68**, 75 (1992).
[7] K. Jacobs, S. Herminghaus, and K. R. Mecke, Langmuir **14**, 965 (1998).
[8] P. Colinet, J. C. Legros, and M. G. Velarde, *Nonlinear Dynamics of Surface-Tension-Driven Instabilities* (Wiley-VCH, Berlin, 2001).
[9] J. P. Burelbach, S. G. Bankoff, and S. H. Davis, J. Fluid Mech. **195**, 463 (1988).
[10] J. P. Burelbach, S. G. Bankoff, and S. H. Davis, Phys. Fluids A **2**, 322 (1990).
[11] A. Oron, Phys. Fluids **12**, 1633 (2000).
[12] M. Bestehorn, A. Pototsky, and U. Thiele, Eur. Phys. J. B **33**, 457 (2003).
[13] R. J. Deissler and A. Oron, Phys. Rev. Lett. **68**, 2948 (1992).
[14] A. Vrij, Discuss. Faraday Soc. **42**, 23 (1966).
[15] L. M. Pismen and Y. Pomeau, Phys. Rev. E **62**, 2480 (2000).
[16] M. Bestehorn and K. Neuffer, Phys. Rev. Lett. **87**, 046101 (2001).
[17] A. V. Lyushnin, A. A. Golovin, and L. M. Pismen, Phys. Rev. E **65**, 021602 (2002).
[18] A. Oron, Phys. Rev. Lett. **85**, 2108 (2000).
[19] A. A. Golovin, A. A. Nepomnyashchy, and L. M. Pismen, J. Fluid Mech. **341**, 317 (1997).
[20] M. J. Tan, S. G. Bankoff, and S. H. Davis, Phys. Fluids A **2**, 313 (1990).
[21] M. Bestehorn, Phys. Rev. E **48**, 3622 (1993).
[22] K. Eckert, M. Bestehorn, and A. Thess, J. Fluid Mech. **356**, 155 (1998).
[23] D. Semwogerere and M. F. Schatz, Phys. Rev. Lett. **88**, 054501 (2002).
[24] K. B. Glasner and T. P. Witelski, Phys. Rev. E **67**, 016302 (2003).
[25] J. W. Cahn and J. E. Hilliard, J. Chem. Phys. **28**, 258 (1958).